Flow velocity measurements using a spectroscopic laser technique.

Diploma paper

Ulf Westblom

LRAP-40 (1985)

Department of Physics
Lund Institute of Technology

ACKNOWLEDGMENTS

I would like to thank those who in different ways have contributed to this diploma work.

-First of all, my supervisor Professor Sune Svanberg, who has assisted with advice and encouraging support when it has been most needed.

-The graduate students at the Physics Department, who always patiently have been prepared to help.

-The personnel in the workshop who have manufactured the mechanical parts.

Lund Jan.1985

CONTENTS

INTRODUCTION

The measurement of velocities is in many situations of great practical interest, for instance in fields such as fluid mechanics, aero dynamics and combustion science. Unfortunately, conventional methods available such as the use of thermocouples, Pitot tubes and LDA (Laser Doppler Anemometry) suffer from a number of important drawbacks. With thermocouples and Pitot tubes the flow field is disturbed and possibly polluted. In LDA, particles have to be injected in the flow, which may cause problems in highly turbulent flows and in boundary layers close to walls. The techniques mentioned above also have the disadvantage that they only provide the velocity at a single point at a time. The technique described in this Diploma work circumvents these problems. It is non intrusive and allows for simultaneously multiple-point velocity measurements in flowing gas. The first imaging measurements of species concentrations using this technique were reported for OH (Ref. 5), while measurements of temperature were described for an In seeded flame (Ref. 6). Such one dimensional (1-D) measurements have been extended to C_2 using single-photon excitation and to O and CO using two-photon excitation. (For a review see Ref. 7). Two-dimensional (2-D) imaging has also been developed using a sheet of exciting laser light in conjunction with a vidicon or diode matrix detector (Ref. 8,9). Imaging measurements of hypersonic flows using LIF in Na atoms (Ref. 10) and I_2 molecules (Ref. 11) have been reported. For imaging measurements on sub-sonic flows and more quantitative velocity assessment a modulation technique with laser beams sent alternately in counter propagating directions has been introduced by Hiller et al. (Ref. 12). This method that was also conceived at Lund Institute of Technology is described in this Diploma paper. In the approach reported here a single-mode laser is fixed in terms of frequency in the wing of a Doppler broadened profile of a seed molecule (I_2), close to the point with maximum slope. By chopping the beam and alternatingly sending it towards /along the flow, a shift out from the line center and a shift in towards the line center is obtained when the gas is moving. For the beam with a shift in towards the line center the LIF (Laser-Induced Fluorescence) will increase while the LIF will decrease for the

beam with a shift out from the line center. The change in intensity is detected perpendicularly to the beam with a photomultiplier tube for single point measurements and with a diode array for multiple point monitoring. Since the intensity changes are directly proportional to the Doppler frequency shift induced by the flow, the velocity can be calculated.

DOPPLER THEORY

If a light source is moving with a velocity in the line of sight equal to $v \cos\theta = v_x$, the frequency detected by a stationary observer appears shifted compared with the frequency ν of the source at rest. This shift $\Delta\nu$, is called the Doppler shift and is given by the expression

$$\Delta\nu = \frac{v_x}{c}\,\nu \qquad (1)$$

where ν is the frequency detected when at rest and c the speed of light. In a gas, where all the atoms move with different velocities and in different directions this effect leads to a broadening of the detected signal. In order to derive the resulting intensity distribution as a function of frequency it is assumed that the velocities in the gas have a Maxwellian distribution and hence given by

$$f(v) = \frac{M}{2RT}\exp\left(-\frac{M}{2RT}\,v^2\right) \qquad (2)$$

where M is the molecular weight, R the gas constant and T the temperature. The number of atoms with a velocity component in the direction of measurement between v and v+dv is $dN=Nf(v)dv$, where N is the total number of emitting atoms. If $Pd\nu$ is the light power emitted in the frequency band between ν and $\nu+d\nu$ and this is proportional to the number of emitting atoms with a velocity component v between v and v+dv the following expression is obtained

$$Pd\nu = k\,N\,f\left(c\,\frac{\nu-\nu_0}{\nu_0}\right)\,c\,\frac{d\nu}{\nu_0} \qquad (3)$$

Integration of this expression gives

$$P = k'f\left(c\,\frac{\nu-\nu_0}{\nu_0}\right) = k''\exp\left(-\frac{M\,c^2}{2RT}\left(\frac{\nu-\nu_0}{\nu_0}\right)^2\right) \qquad (4)$$

Equation (4) describes the broadening caused by atomic motion when the atoms emit light of one single frequency. Since the atoms have a natural frequency distribution, given by the Lorentzian expression

$$L(\nu) = I_0\,\frac{1}{1+\left(\frac{2(\nu-\nu_0)}{\Delta\nu}\right)^2} \qquad \Delta\nu = \frac{1}{2\pi\tau} \qquad (5)$$

due to their finite lifetime in the excited state, the complete contour of the line will be determined by the combined effect of Doppler and radiation broadening. Eq. (5) gives the intensity at a frequency ν, without taking the Doppler broadening into account. Since all the frequencies emitted will be affected by the Doppler broadening the result for a given frequency $\nu - \delta$ will be Eq. (5) multiplied by the Doppler function (4) with the frequency difference δ. The resulting intensity function is then

$$I(\nu) = \int L(\nu - \delta)\, P(\delta)\, d\delta \qquad (6)$$

This folding integral, known as a Voigt profile, has no analytical solutions, but numerical solutions have been tabulated. However, a more important contribution to the total broadening of the profile is frequently given by unresolved hyperfine structure and in practice such structure is completely decisive for the profile's shape and width. The final profile is given by the Doppler function weigthed against several Lorentz functions, for I_2 15 or 21. In Fig. 1 a recording of the profile for a resonance line in Iodine is shown. Enclosed are also the fringes from a Fabry-Perot interferometer with a free spectral range of 1.5 GHz. Fig. 2 shows for comparison a resolved resonance line in Iodine recorded with high-resolution polarization spectroscopy (Ref. 3).

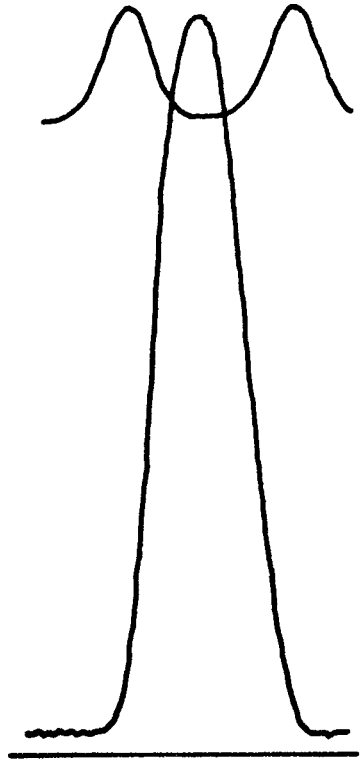

Fig. 1. Recording of a resonance line in Iodine.

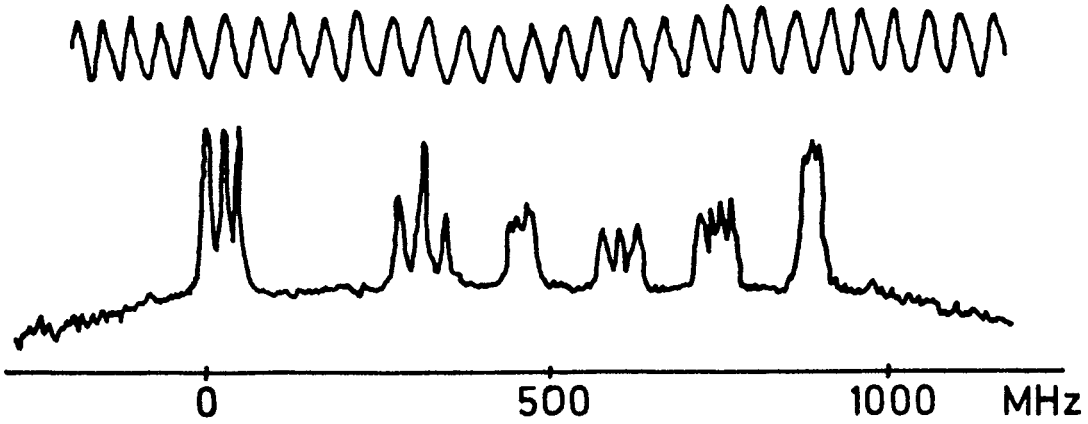

Fig. 2. Resolved resonance line in Iodine recorded with polarization spectroscopy.

THE VELOCITY EQUATION

For non-relativistic velocities the Doppler shift can be written as

$$\Delta\nu = \frac{v}{c}\,\nu \tag{7}$$

or expressed for the velocity

$$v = \frac{c}{\nu}\,\Delta\nu \tag{8}$$

The speed of light c and the laser frequency ν_o can be determined with great accuracy and they are also independent of experimental circumstances. What remains to be determined in order to calculate the velocity is the frequency shift $\Delta\nu$. Assuming that the wing of the Doppler profile is linear for small shifts, $\Delta\nu$ and introducing the lineshape function $I(\nu)$, (See Fig. 3 next page), $\Delta\nu$ can be expressed as

$$\Delta\nu = \frac{I(\nu_o+\Delta\nu) - I(\nu_o)}{\left.\frac{\partial I}{\partial\nu}\right|_{\nu=\nu_o}} \tag{9}$$

By normalizing $I(\nu)$ to unity at the line center, setting $I(\nu_m)=I_m$ and using Eq. (8) we can rewrite Eq. (9)

$$v = \frac{c}{\nu}\,\frac{g(\nu_o+\Delta\nu) - g(\nu_o)}{\left.\frac{\partial g}{\partial\nu}\right|_{\nu=\nu_o}} \tag{10}$$

This form has the disadvantage of requiring the fluorescence intensity to be measured at two different frequencies, which means, that the laser frequency must be changed while performing measurements. This can be avoided by using two counter-propagating beams giving the fluorescence intensities I_l at $\nu_o+\Delta\nu$ and I_r at $\nu_o-\Delta\nu$. Using I_l and I_r, we can write

$$g(\nu+\Delta\nu)-g(\nu_o) = (I_l - I_r)/(2I_m) \tag{11}$$

Considering further that I_o/I_m represents the value of $g(\nu)$ at ν_o and that $I_o=(I_l+I_r)/2$, Eq. (10) can be written in its final form

$$v = \frac{c}{\nu}\,\frac{I_l - I_r}{I_l + I_r}\,\frac{g(\nu_o)}{g(\nu_o)} \tag{12}$$

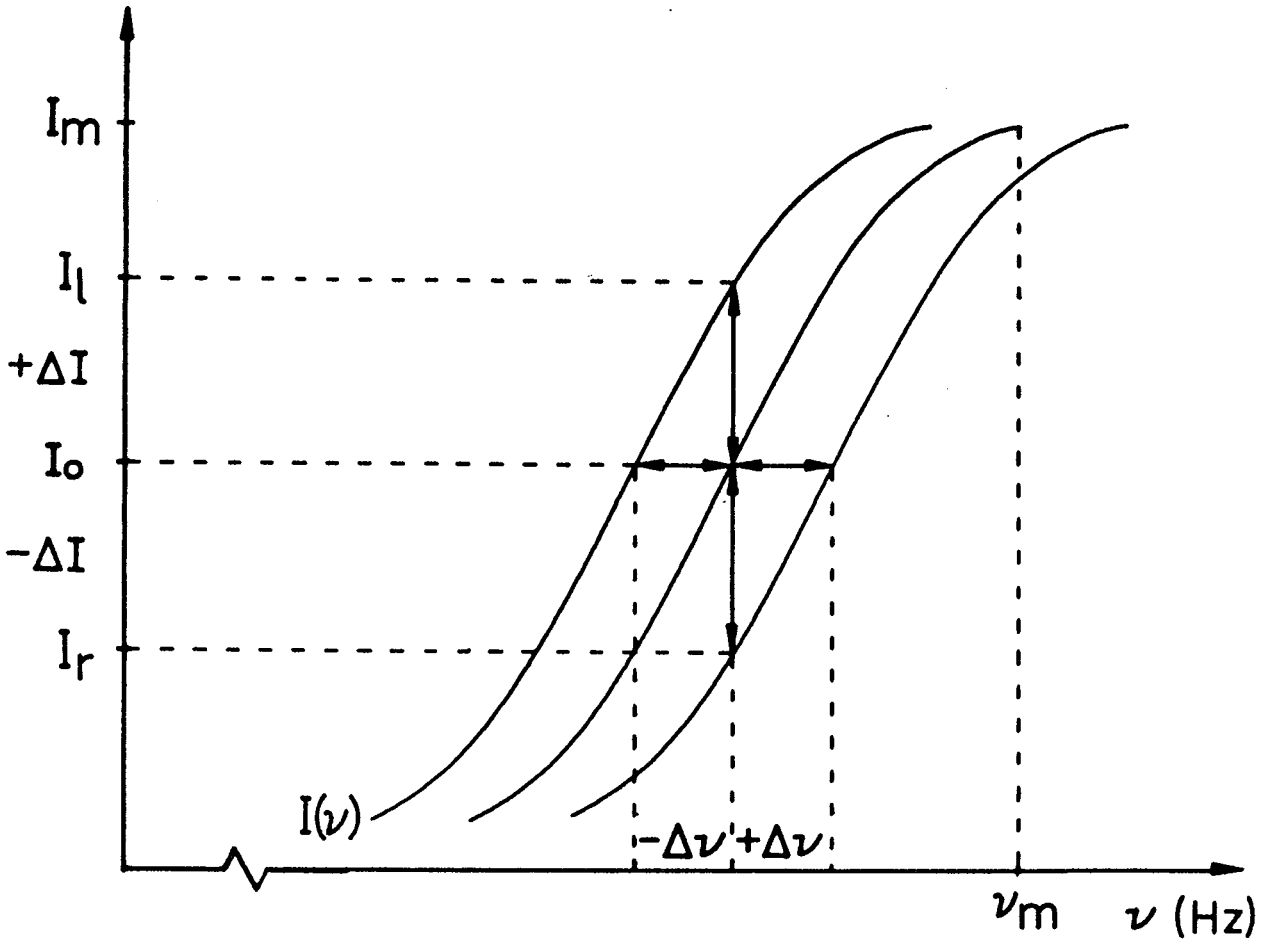

Fig. 3. Illustration of the principle of spectroscopic velocity measurements.

The use of two counter propagating beams thus increases the sensitivity by doubling the frequency shift and eliminates the need to determine seeding fraction, quenching factor and line strength. The velocity equation can be separated into two parts, A and B, where

$$A = \frac{c}{\nu} \frac{g(\nu)}{g'(\nu)} \quad (13) \quad \text{and} \quad B = \frac{I_l - I_r}{I_l + I_r} \quad (14)$$

so that once the laser frequency has been set in the wing of a line, the velocity is only a function of terms in B. The profile function and its first derivate, can be found either theoretically from a Voigt function using known broadening coeffiecients or, as here, experimentally by measuring the line shape in a static cell.

the value of k can be calculated. With $g(\nu)=\exp(-k(\nu_0-\nu)^2)$, the ratio $g(\nu)/g'(\nu)$, reduces to $(2k(\nu_0-\nu))^{-1}$ and the intensity independent term $(cg(\nu))/(\nu_0 g'(\nu))$ can now be evaluated. Measurements in Fig. 10 give 2 HWHM=0.88 GHz and with λ=5892.34 Å and assuming that the laser frequency has been set close to the point at half heigth ($\nu_0-\nu = \Delta\nu/2$) one gets $c/(\nu_0 2k(\nu_0-\nu))= (\nu_0\Delta\nu)/(4\ln 2)$=C=188 m/s. The intensity term $(I_l-I_r)/(I_l+I_r)$ is always smaller than one, so C is clearly the highest velocity that can be aquired. A direct geometrical measurement of the factor $g'(\nu)$ gives with $g(\nu)$=0.5, C=154 m/s. Fig. 14 shows two LIF recordings made with the nozzle arrangement shown in Fig. 15 and underneath the velocity distribution calculated with Eq. (12) is given.

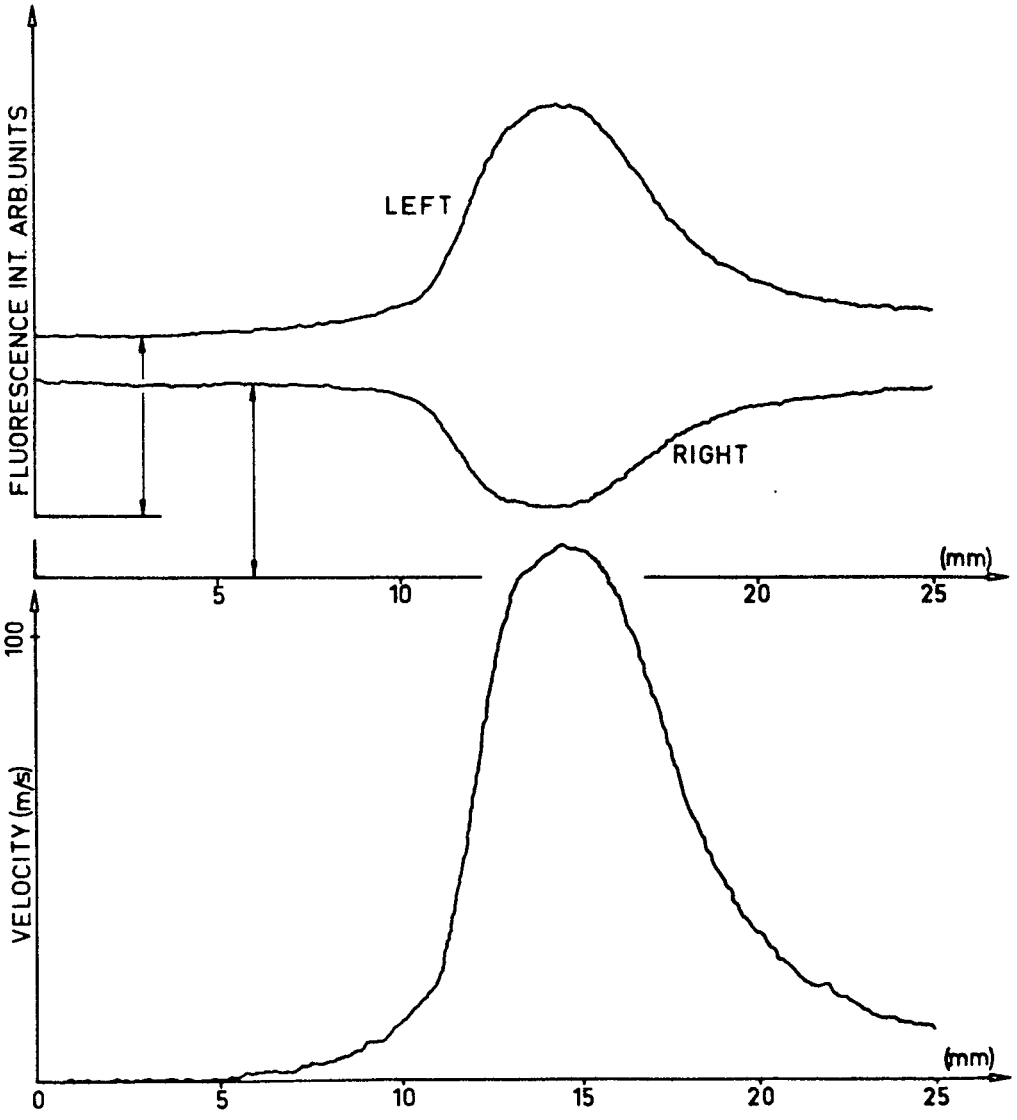

Fig. 14. Fluorescence light spatial distribution for laser beams propagating from the left and from the right, and the velocity distribution calculated from these distributions using Eq. (12). The chamber pressure was 1 torr and the recording time for each LIF distribution was 2.6 ms.

EXPERIMENTAL SETUP

Two different experimental arrangements were used, both schematically shown in Fig. 4. A single-mode dye laser (Coherent 599) with Rhodamine 6G dye, was pumped by an Ar^+ laser (Spectra Physics 171), yielding a typical output of 100 mW. For monitoring purposes parts of the beam were deflected via three beam-splitters (a,b,c). The first (a) of the deflected beams was directed to a scanning Fabry-Perot interferometer, which allowed for control of the mode structure of the laser. The second (b) was split again; one beam going to a photo diode measuring laser intensity, the other beam going through a cell containing Iodine. The LIF from the cell was measured by a photomultiplier tube. By measuring both the laser intensity and the LIF intensity it was possible to determine whether a change in signal was due to frequency drifts or a laser intensity change. The signal from the static cell was also used for setting the frequency at the right position in the wing of the line. A third beam (c) could be deflected to a digital wavelength meter, giving the frequency with high accuracy. The main beam was sent through a rotating mirror wheel which directed it alternatingly to (d) and (e) Inside the cell, two 90^0 prisms linked the beam alongside the nozzle. The nozzle, which was a tapered glass tube with an orifice diameter of 0.5 mm, was connected to a seeding chamber, containing Iodine crystals at room temperature, and a flow meter. The reason for choosing Iodine as seeding molecule was that it is non-perturbing to the flow field since it can be added at room temperature, it has a broad visible absorbtion spectrum easily accessible by laser sources and it provides strong fluorescence signals. The flow rate was regulated with a needle valve (f) and the flow chamber could be shut of from the seeding chamber with a valve (g) to prevent Iodine from diffusing into the flow chamber while not performing measurements. The cell was evacuated with a rotary vacuum pump to a pressure down to 1 torr.

POINT MONITORING SYSTEM

In the setup marked POINT MONITOR in Fig. 4 the beam was chopped at 75 Hz by a sectorially aluminized quartz disc and the LIF was projected on the entrance slit of a 0.5 m monochromator (Bausch& Lomb), equipped with a photomultiplier tube. The signal from the photomultiplier tube was recorded with a lock-in ampli-

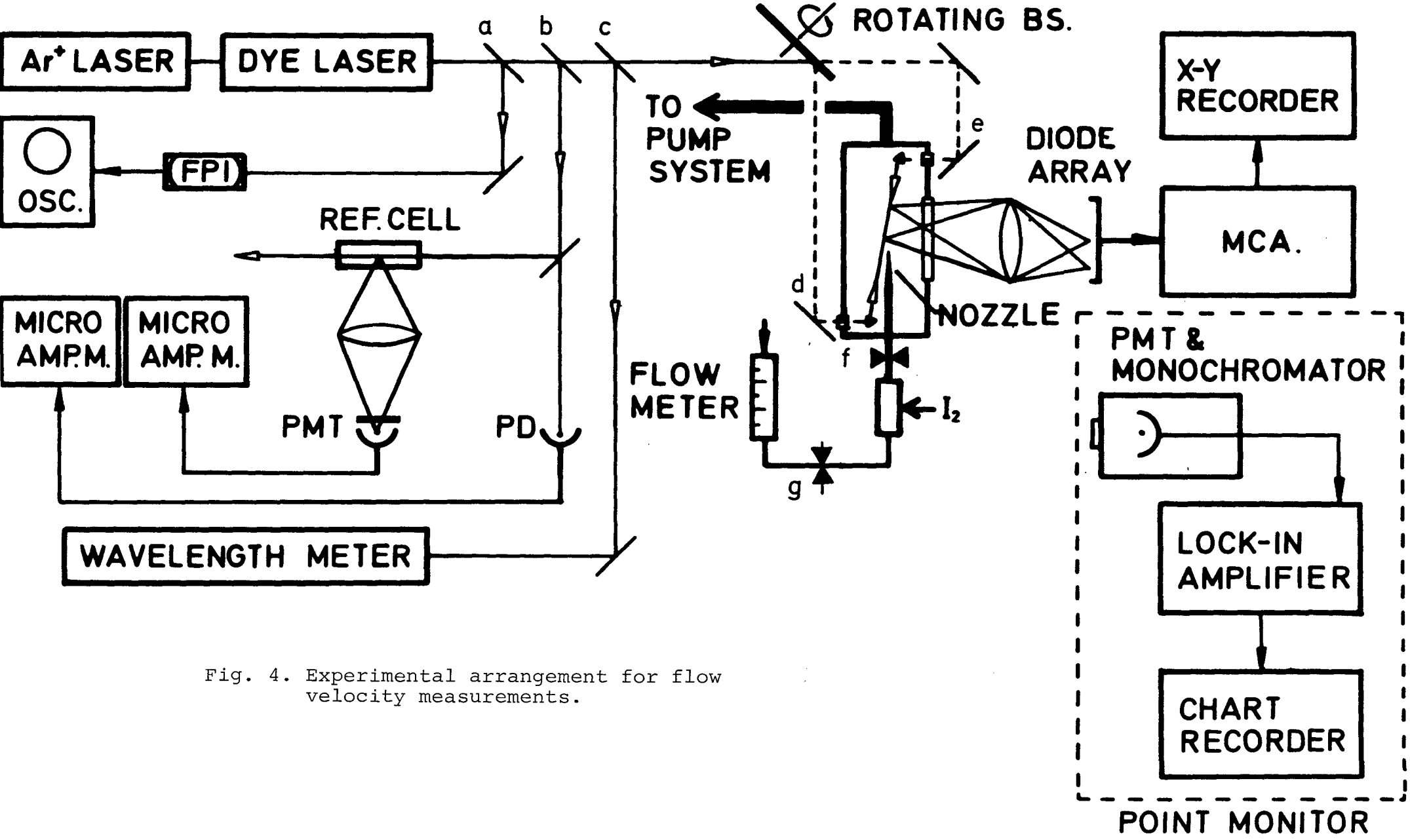

Fig. 4. Experimental arrangement for flow velocity measurements.

fier (PAR HR-8) with a reference signal taken from the chopper wheel. In this set-up the lock-in amplifier receives two signals, both on the frequency 75 Hz, one from each of the two counter propagating beams, with a relative phase difference of 180°. If the gas is not moving and the beams are balanced to yield equal fluorescence intensities, the signals will average to a net of zero. However, when the gas is moving, the LIF from the beam shifting in towards the line center will increase, while the LIF from the beam shifting out from the line center will decrease. The net result will be a signal equal to $(I_l - I_r)$. Examples of this signal type are shown in Fig. 5. If the frequency is set in the other wing of the profile at the same height the signal will change signs as demonstrated in the figure. With this detection method, only the difference, $(I_l - I_r)$ is aquired, but by blocking one of the beams the full signal, I_l or I_r, can be measured. This method method does not provide spatial resolution but was used to gain experience with the technique.

DIODE ARRAY SYSTEM

In this setup a segment of the beam was projected on a diode array, connected to a Tracor Northern-1710 main frame, on which data was processed and stored. The diode array was a Tracor Northern Model TN-1223-4IG with a light sensitive area of (25 x 2.5)mm and 1024 individual elements. The chopper wheel was moved manually between the exposures.

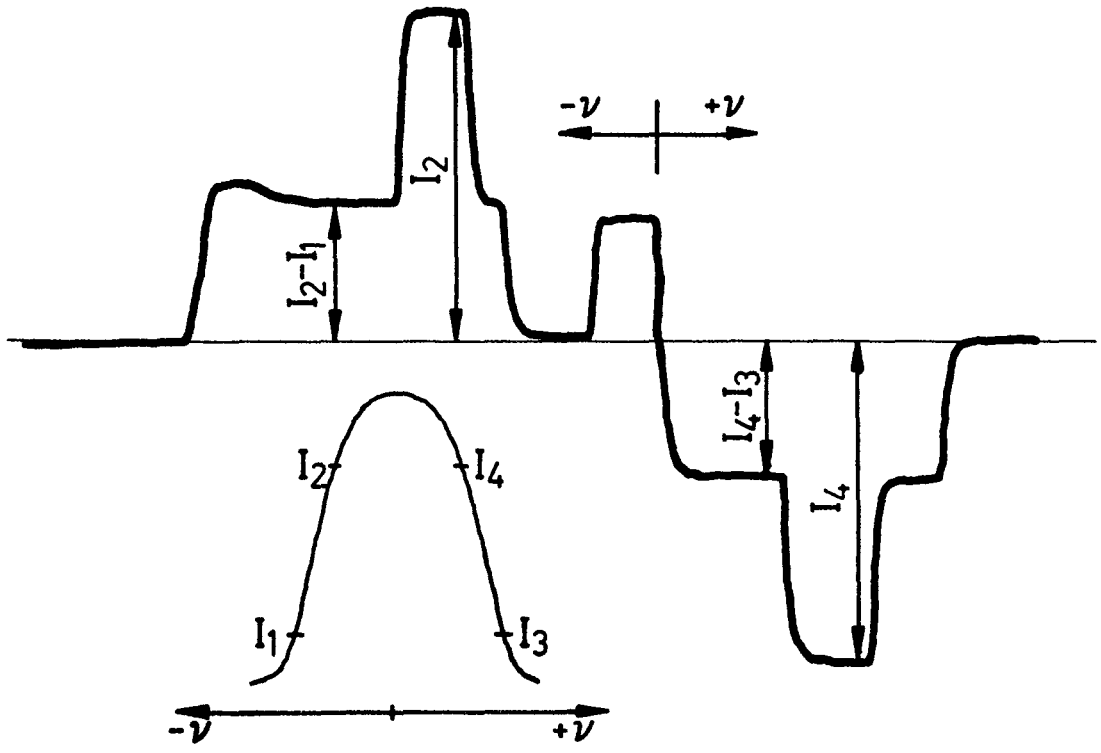

Fig. 5. Signal obtained with lock-in technique.

EXPERIMENTAL RESULTS

In the following, only recordings made with the diode array set-up will be discussed since these are the most interesting. In order to eliminate effects of straylight in the cell and non-linearities in the diode array the following exposure scheme has been used for every recording

$$\text{Right signal} = \frac{\text{Right beam, flow on} - \text{Right beam, background}}{\text{Right beam, flow off} - \text{Right beam, background}}$$

$$\text{Left signal} = \frac{\text{Left beam, flow on} - \text{Left beam, background}}{\text{Left beam, flow off} - \text{Left beam, background}}$$

The background exposures were made with the frequency set off the line. The exposure time for all recordings were 2.6 ms. The position of the nozzle with respect to the to beam for the recordings in Fig. 8-12 is shown in Fig. 6.

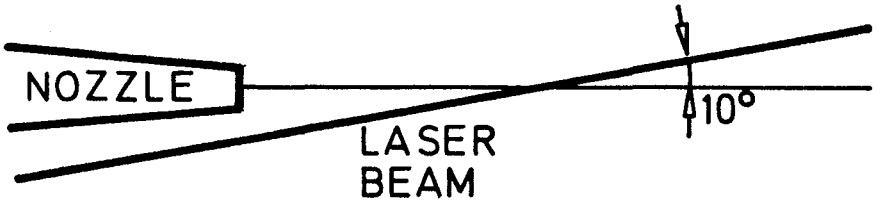

Fig. 6. Position of the nozzle with respect to the beam.

Some of the underlaying phenomena in the recordings should first be discussed in order to make a correct interpretation possible.

1. When the valve is opened and air starts flowing into the flow chamber the Iodine concentration increases. Since the Left and the Right recordings were not made simultaneously the average background concentration was higher for the latter exposure resulting in different relative LIF intensities in non flowing areas. This can be seen in the figures where the curves do not overlap behind the nozzle.

2. If the beams do not overlap completely in space the fluorescence recorded will describe the frequency shift in different areas and hence measure different velocity distributions. The effect of this can be seen in the figures where the Left signal maximum does not occur at the same position as the Right signal minimum. The same problem will arise if the two beams have

different diameters.

3. One could expect that the two beams should be symmetrical with respect to each other. As can be seen in the figures this is clearly not the case. The most plausible cause for this phenomenon is that the Iodine concentration is higher in the jet than in the rest of the cell. Therefore the LIF for the Left beam does not only increase because of the frequency shift but also because of the higher Iodine concentration. For the Right beam the situation is the opposite, the higher Iodine concentration compensates for part of the decrease in intensity due to the frequency shift. However, the velocity equation, Eq. (11) is independent of the seeding concentration so this does not affect the measurements.

The high signal-to-noise ratio in the recordings is clearly a result of the low pressure at which the recordings were performed. At higher pressures the LIF intensity decreases due to quenching. A recording of the pressure dependence of the LIF is shown in Fig. 7. Recordings made at higher pressures, 50 torr and 100 torr, are shown in Fig. 10 and in Fig. 11. However, by increasing the exposure time, which also for these recordings was 2.6 ms, the signal-to-noise ratio can be improved.

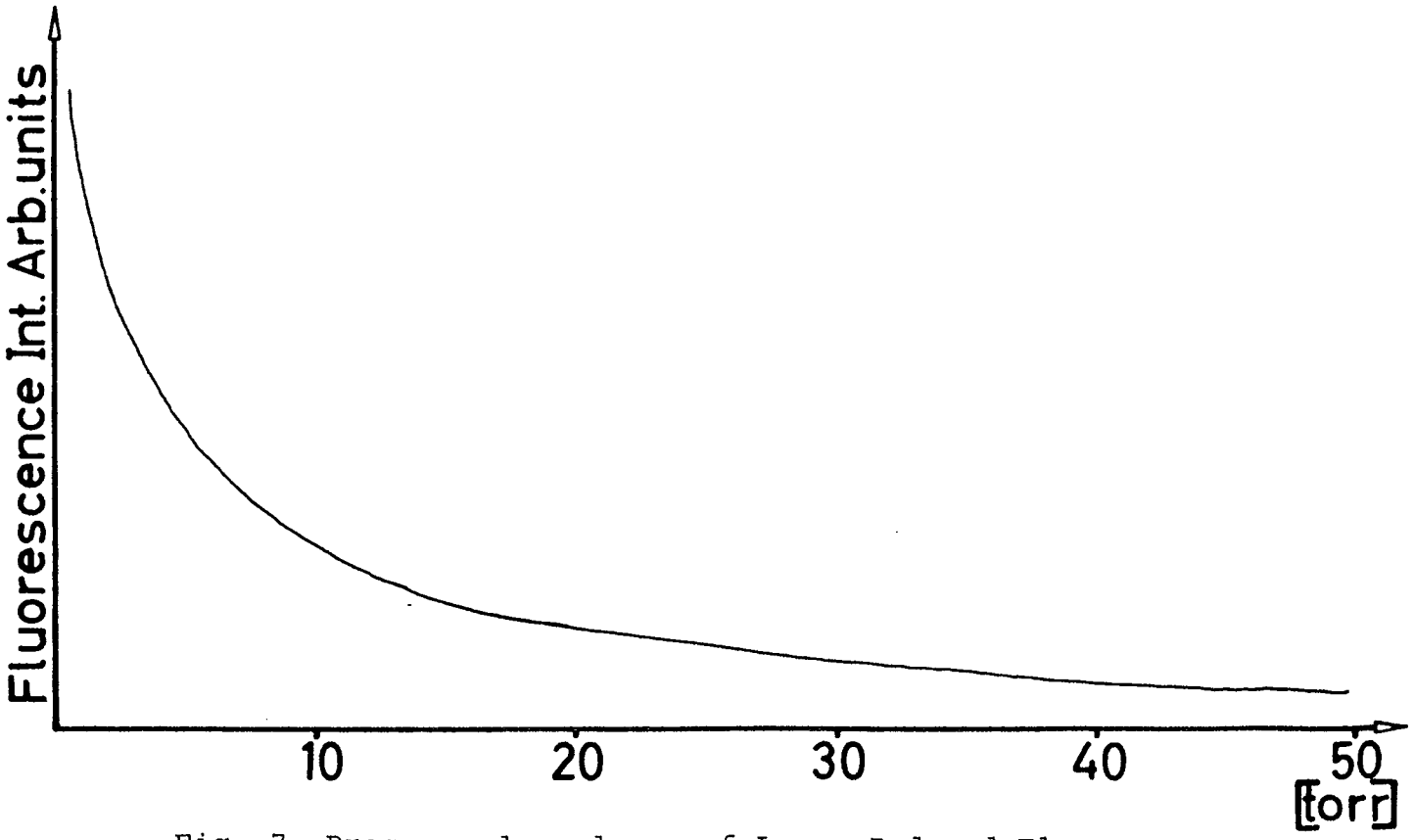

Fig. 7. Pressure dependence of Laser-Induced Fluorescence.

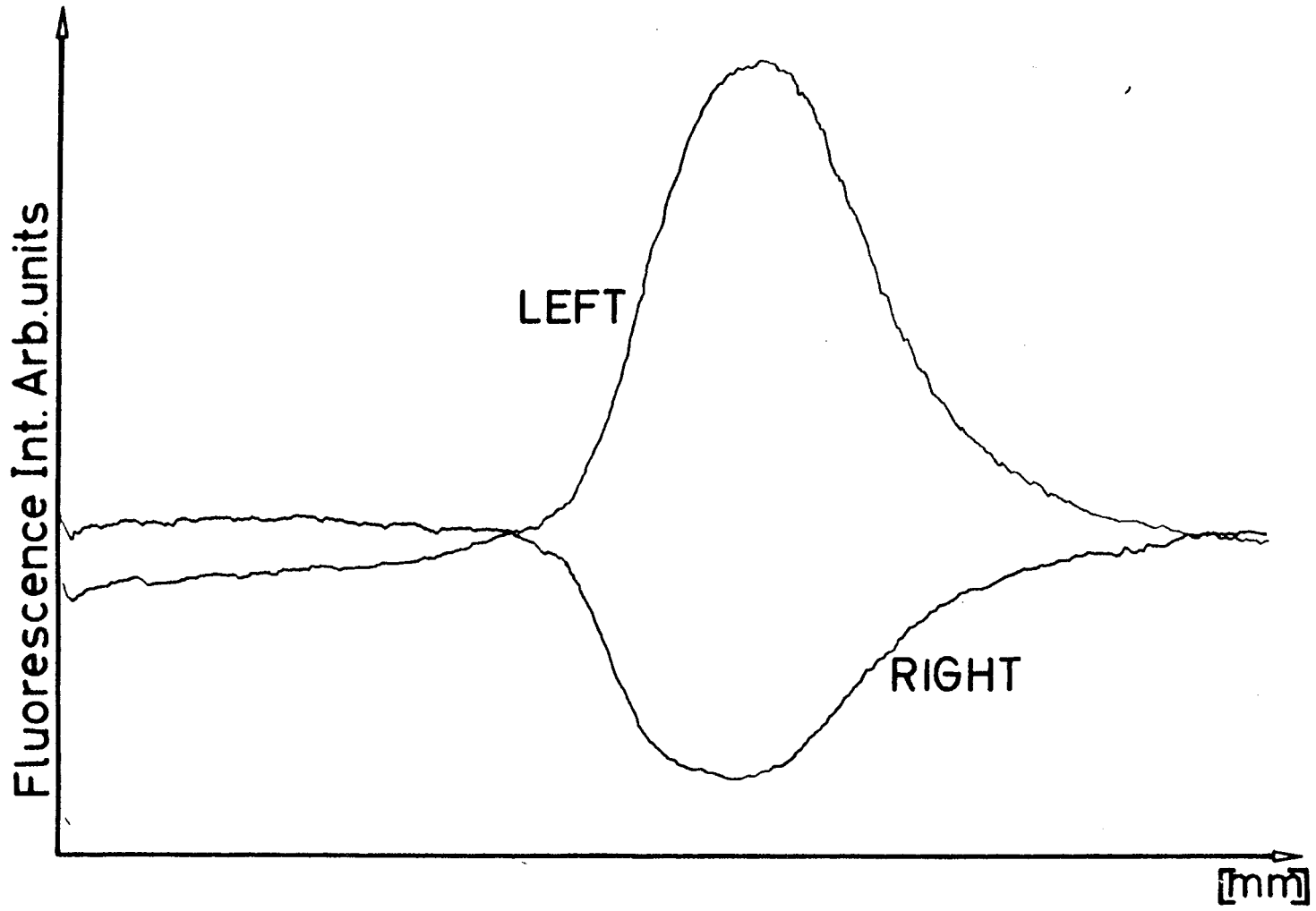

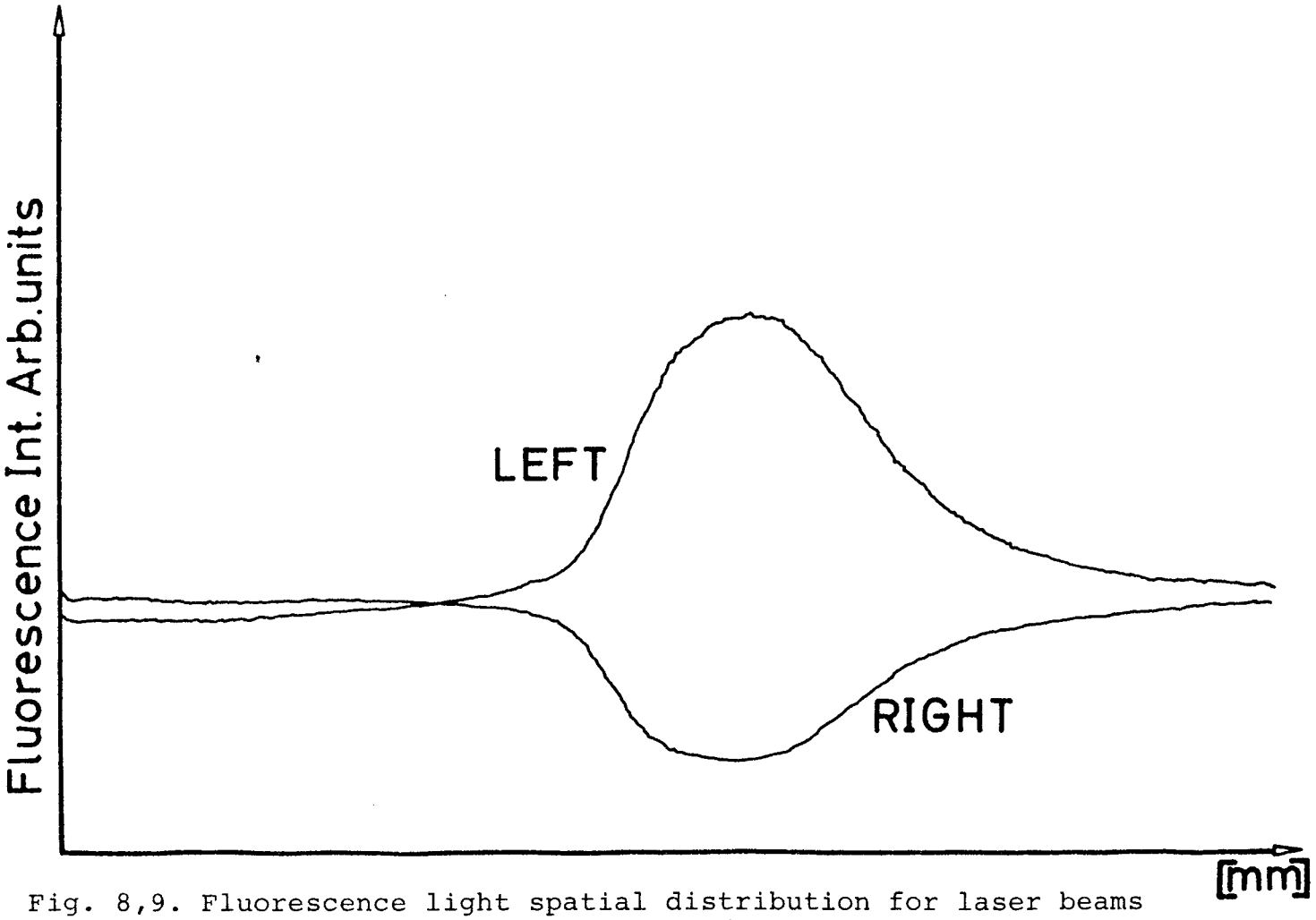

Fig. 8,9. Fluorescence light spatial distribution for laser beams propagating from the left and from the right. The chamber pressure was 1 torr and the recording time for each LIF distribution was 2.6 ms. In Fig. 9 the distance nozzle-beam is greater than in Fig. 8.

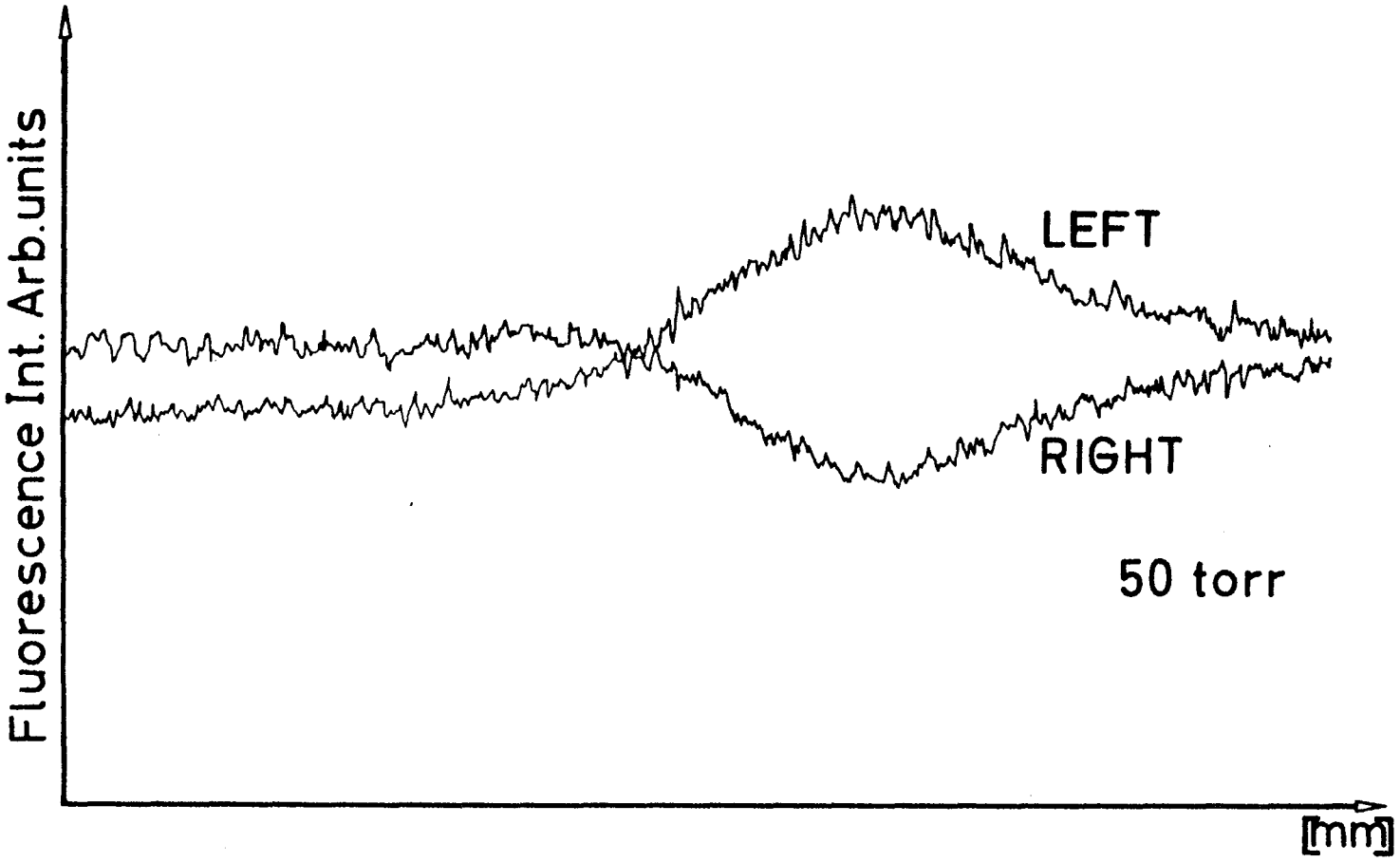

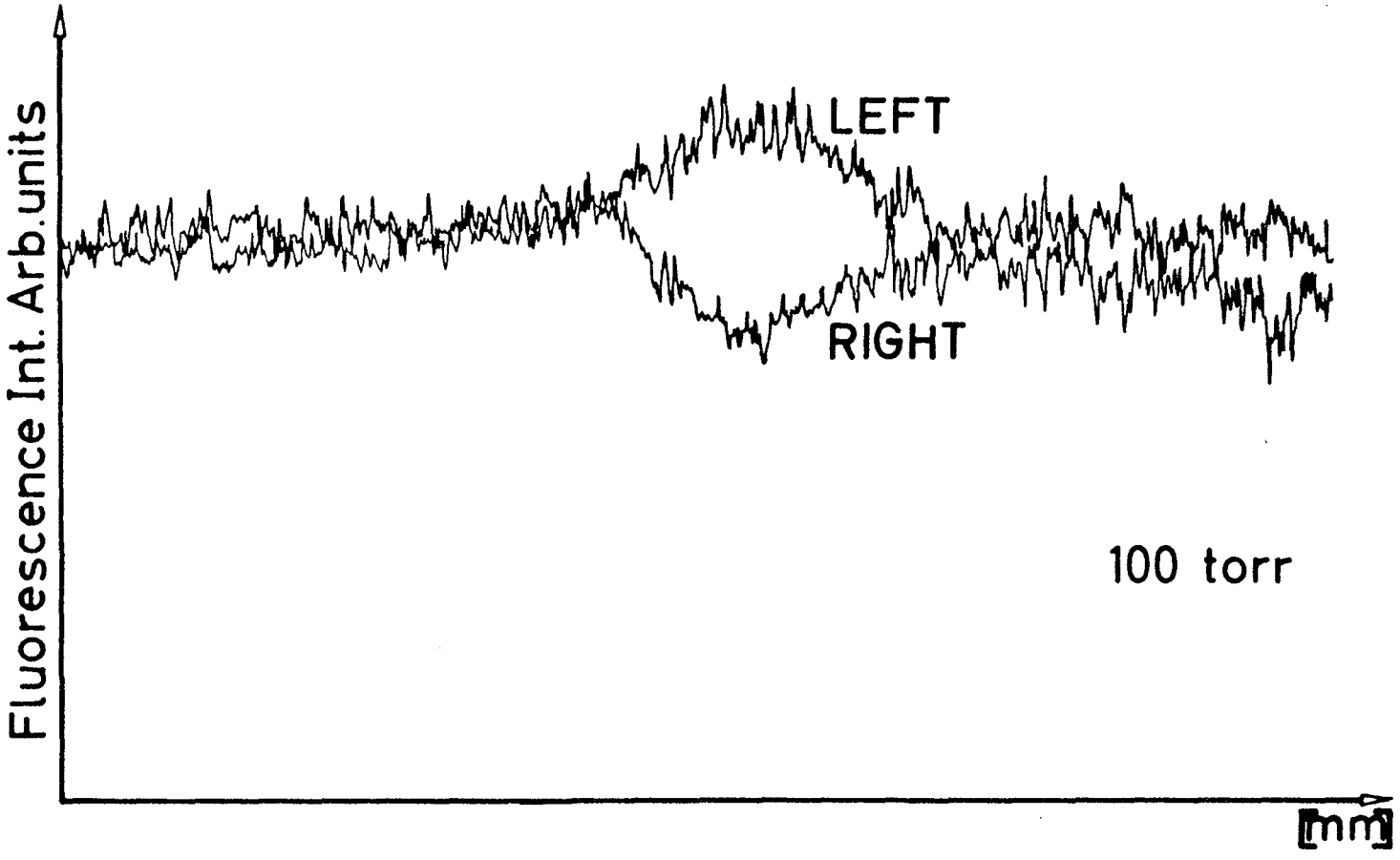

Fig. 10,11. Fluorescence light spatial distribution for laser beams propagating from the left and from the right. The chamber pressure was in Fig.10, 50 torr and in Fig. 11, 100 torr. The recording time for each LIF distribution was 2.6 ms.

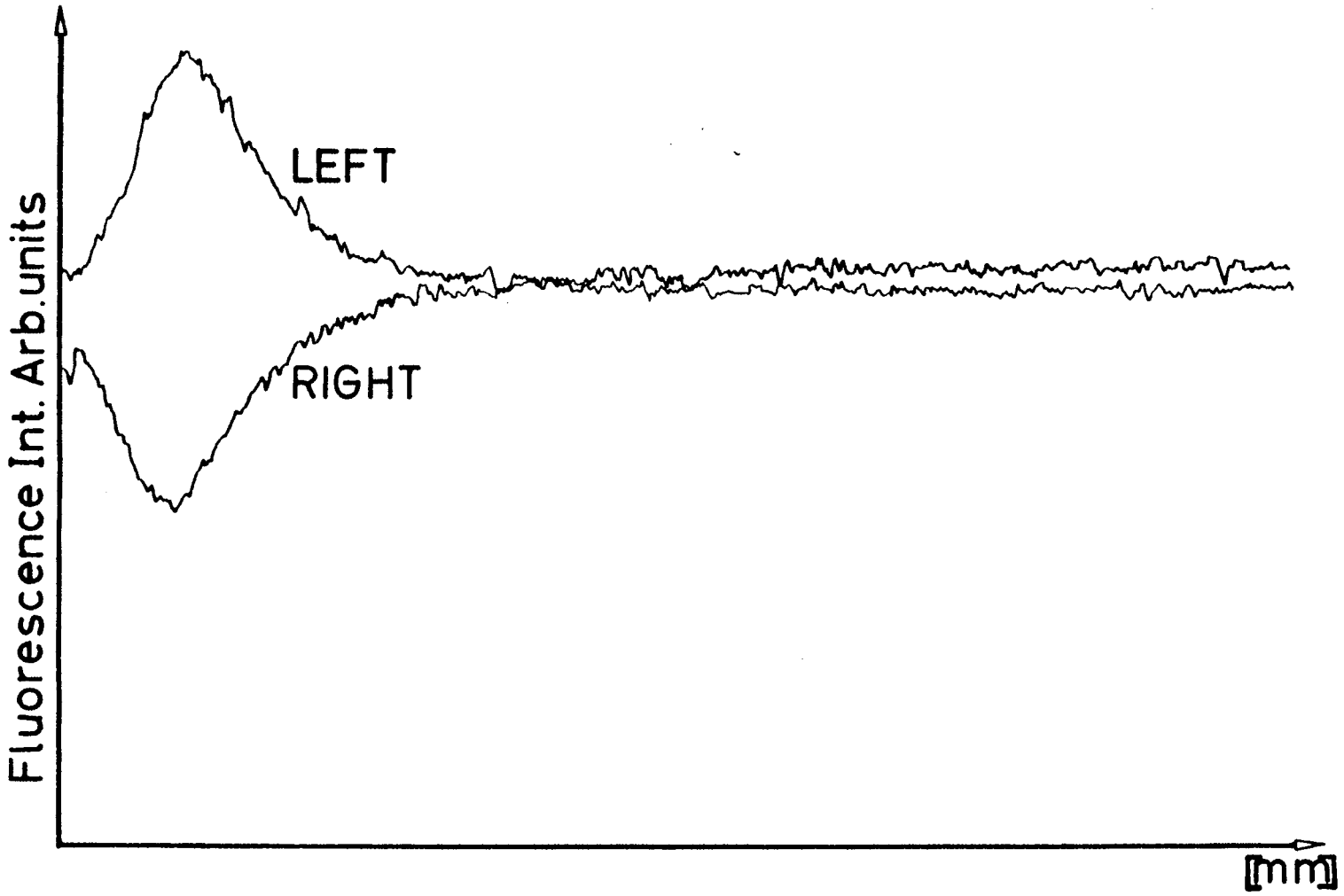

Fig. 12. Fluorescence light distribution recorded with a different nozzle arrangement shown for comparison.

CALCULATIONS

Using Eq. (12) derived on pages (7-8), the velocity distribution for one of the recorded flows will be calculated. First a value of the frequency dependent term $(cg(\nu))/(\nu_o g'(\nu))$ must be determined. As mentioned before this can be done in several different ways. Here we will first fit a theoretical Doppler curve, a Gauss function, to a recorded line profile and then compare with a direct measurement of the slope on the recorded line. Fig. 13 shows a recorded line profile and a plotted Gaussian for comparison. As can be seen they do not overlap completely, which also should not be expected considering that the line, as earlier described, consists of several unresolved sublines. Of course, since the number of lines under the Doppler broadened profile can be determined and the mathematical expressions for the different broadening effects are known, a more elaborate calculation can be done in order to derive an expression better describing the lineshape. However, it should be noticed that the lineshape, $g(\nu)$ is both pressure and temperature dependent and therefore should be recorded at conditions equal to those in the flow. Enclosed in the figure are also fringes from a Fabry-Perot interferometer with a free spectral range of 1.5 GHz. With this as a recording reference, the HWHM (Half Width at Half Maximum) can be estimated. A theoretical Doppler curve normalized to unity at the line center, is as has been shown on pages 5-6 given by

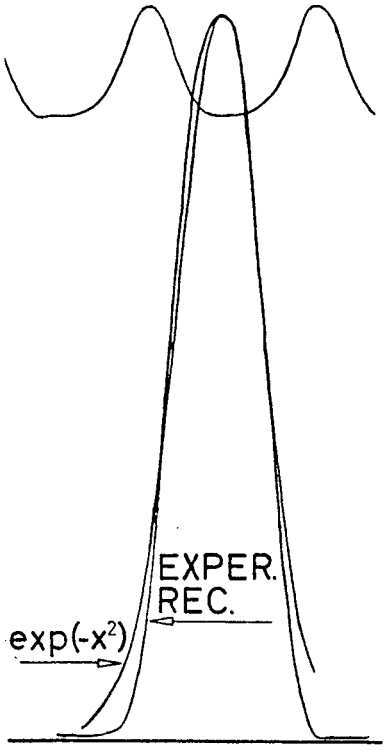

Fig. 13. Comparison between a recorded Iodine line and a plotted Gaussian.

$$f(\nu) = \exp(-k(\nu - \nu_o)^2) \quad \text{with } k = \frac{M c^2}{2RT} \tag{15}$$

The HWHM for this curve becomes

$$\Delta\nu = (\ln 2/k)^{0.5} \tag{16}$$

By setting Eq. (16) equal to the HWHM as measured on the profile

It is often interesting to compare the results from different methods. A flow theoretical analysis (Ref. 13) gives the following equations

$$u_c = u_o \, 6.4 \, \frac{D}{x} \tag{17}$$

$$u = u_c \left[1 + \frac{1}{0.0157 \, x^2} \right] \tag{18}$$

$$a = \sqrt{k \, R \, T} \tag{19}$$

where Eq. (17) gives the velocity on the symmetry axis as a function of the distance from the nozzle orifice, Eq. (18) the velocity distribution for fixed x as a function of r, the peripendicular distance from the symmetry axis and Eq. (19) the velocity of sound as a function of temperature. U_o is the velocity at the orifice, other variables are explained in Fig. 15.

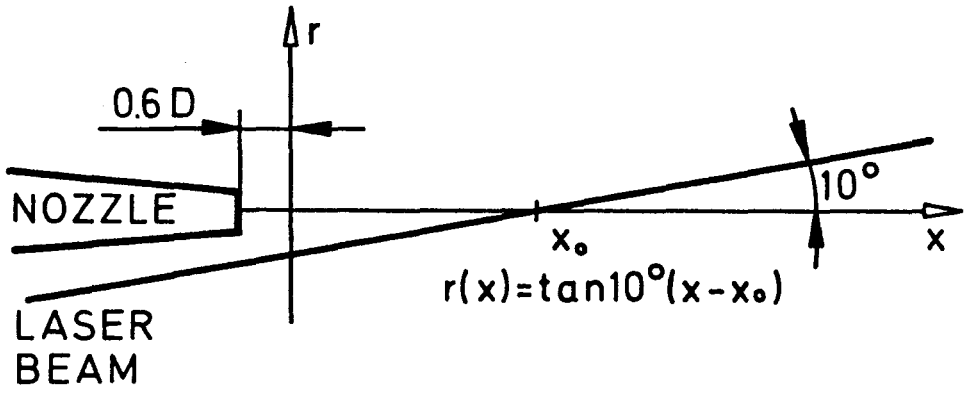

Fig. 15. Position of the nozzle with respect to the beam.

In Eq. (17) and in Eq. (18), x is measured from a point 0.6D down stream from the nozzle. Due to the large pressure fall over the nozzle (759 torr) the velocity at the nozzle orifice is Mach one (Ref. 13) and hence, $u_o = a$. This combined with Eq. (17),(18) and the fact that $r(x) = \tan 10^\circ (x - x_o)$ along the beam gives

$$u = u_o \, 6.4 \, \frac{D}{x} \left[1 + \frac{\tan^2 10^\circ}{0.0157} \left(1 - \frac{x_o}{x} \right)^2 \right]^{-2} \tag{20}$$

For air k=1.4 and R=287 wich gives u_o=344m/s. In Fig. 16, u(x) is plotted and compared with an experimentally acquired velocity distribution, calculated with Eq. (11) and using data from the recording in Fig. 14. The heights of the curves have been adjusted to match. The maximum velocity calculated with Eq. (20) is u_{max} =105m/s. The experimental data gives with C=154, u_{max}=109m/s

and with C=188, u_{max}=133m/s. However, as seen in Fig. 16, the agreement is not so good for other distances from the nozzle.

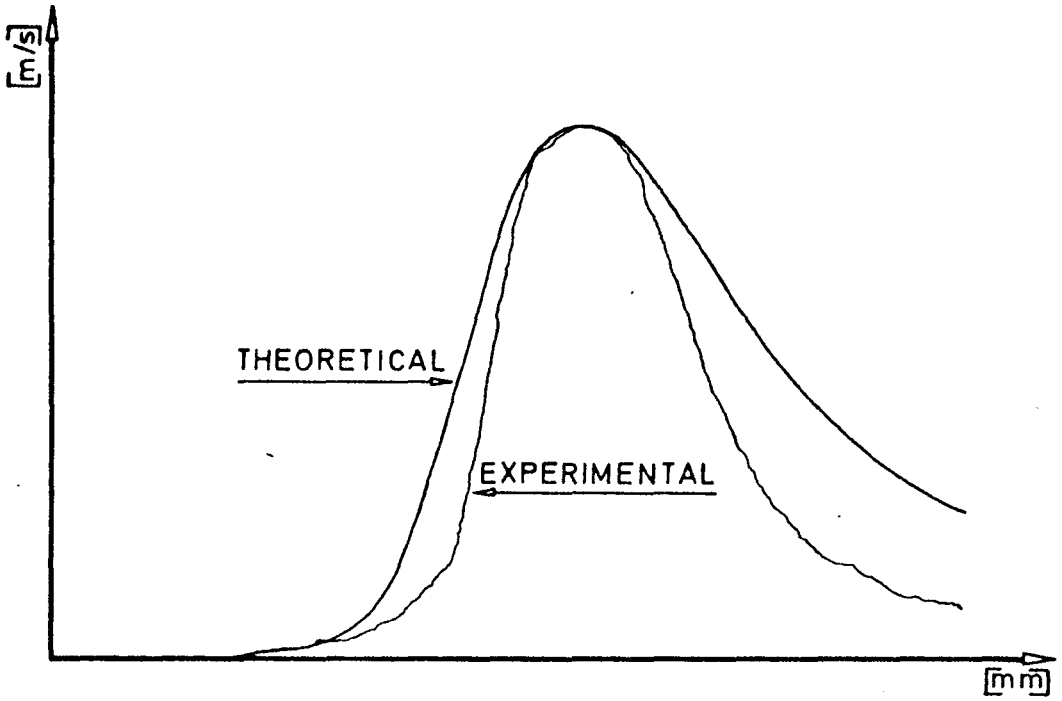

Fig. 16. Comparison between an experimentally obtained velocity distribution and one obtained from theoretical flow equations.

However, it should be pointed out that the main aim of this work has not been to make exact measurements but to gain general experience with the technique. Therefore the experimental set-up used has not been designed to allow for a more accurate determination of the parameters needed to calculate the velocity. This is especially true for the spectroscopic factor $g(\nu)/g'(\nu)$. Clearly, the problems in determining this factor accurately is one of the weak points in this technique and in order to make it a realistic alternative for velocity measurements, attention should, in the development of it, be focused on attempts to overcome them. However, there are good reasons to belive that this can be done and that the technique has the potential to become a valuable tool for velocity measurements.

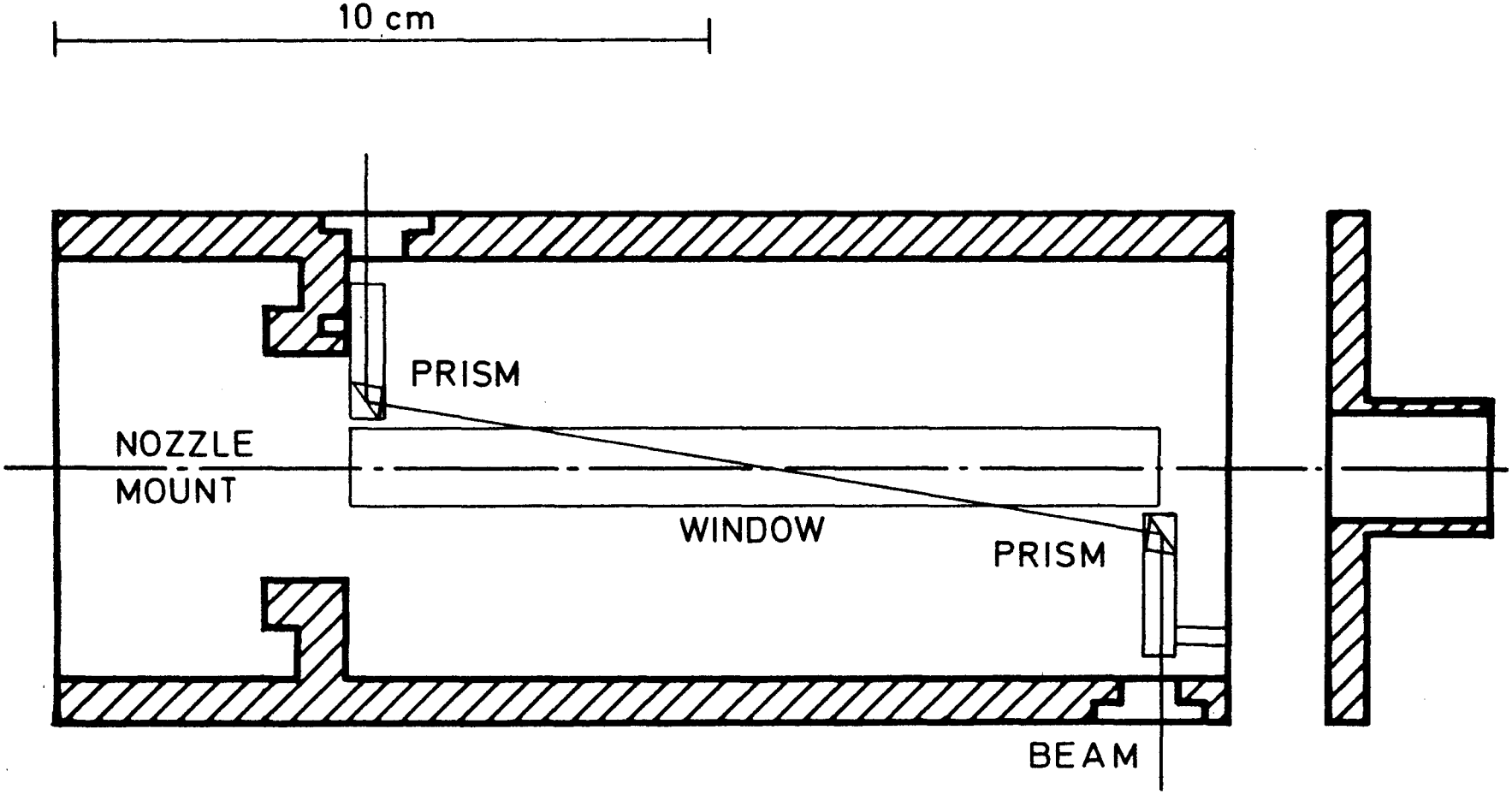

Cross section of flow chamber showing position of the prisms and the window.

REFERENCES

1. Kuhn, H.G., Atomic Spectra, Longmans,1962.

2. Drain, L.E., The laser Doppler technique, John Wiley&Sons, 1980.

3. Grafstrom, P., Levinsson, C. and Svanberg, S., Göteborg Insitute of Physics Reports GIPR-166 (1978)

4. Sune Svanberg, Atom och Molekylspektroskopi, Lund 1982.

5. Alden, M., Edner, H., Holmstedt, G., Svanberg, S., and Högberg, T., Appl. Opt. 21, 1236 (1982).

6. Alden, M., Grafström, P., Lundberg, H. and Svanberg, S ., Opt. Lett. 8 241 (1983).

7. Alden, M. and Svanberg, S. in Proc. of the ECOOSA `84, to appear, and in Proc. of the ICAELO `84, to appear.

8. Dyer, M.J. and Crosley, D.R., Opt. Lett. 7, 382 (1982).

9. Kyachakoff, G., Howe, R.D., Hanson, R.K. and McDaniel, J.C., Appl. Opt. 21, 3225 (1982).

10. Zimmermann, M. and Miles, R.B., Appl. Phys. Lett. 37, 885 (1980); Cheng, S., Zimmermann, M. and Miles, R.B.,Appl. Phys. Lett. 43, 143 (1984).

11. McDaniel, J.C., Hiller, B. and Hanson, R.K., Opt. Lett. 8, 51 (1983).

12. Hiller, B., McDaniel, J.C., Rea, E.C.,Jr. and Hanson, R.K., Opt. Lett. 8, 474 (1983).

13. Tyllered, G. Fluidmekanik, Lund, 1981.